

See discussions, stats, and author profiles for this publication at: <https://www.researchgate.net/publication/263954611>

Use of Steam Activation as a Post-treatment Technique in the Preparation of Carbon Molecular Sieve Membranes

ARTICLE *in* INDUSTRIAL & ENGINEERING CHEMISTRY RESEARCH · APRIL 2012

Impact Factor: 2.59 · DOI: 10.1021/ie300261r

CITATIONS

3

READS

22

7 AUTHORS, INCLUDING:



Majid Monji

University of Southern California

11 PUBLICATIONS 15 CITATIONS

SEE PROFILE

Use of Steam Activation as a Post-treatment Technique in the Preparation of Carbon Molecular Sieve Membranes

Hui-Chun Lee,[†] Majid Monji,[†] Doug Parsley,[§] Muhammad Sahimi,[†] Paul Liu,[§] Fokion Egolfopoulos,[‡] and Theodore Tsotsis^{*,†}

[†]Mork Family Department of Chemical Engineering and Materials Science and [‡]Department of Aerospace and Mechanical Engineering, University of Southern California, Los Angeles, California 90089, United States

[§]Media and Process Technology, Inc., Pittsburgh, Pennsylvania 15236, United States

Supporting Information

ABSTRACT: Carbon molecular sieve (CMS) membranes have been studied in the past few years as an alternative to both inorganic and polymeric membranes for gas separation under high temperature and pressure conditions. These membranes are made by the pyrolysis of polymeric precursors, and control of their pore size and separation characteristics is accomplished conventionally mainly by choosing the appropriate precursor and by varying the conditions, such as atmosphere, temperature, and duration, of the carbonization procedure. Often, however, the technique does not succeed to consistently provide the tight pore size control required for the separation of important gas pairs, and thus, an additional post-treatment step is needed. In this investigation steam activation was studied as a post-treatment technique in the preparation of CMS membranes. The goal was to adjust the structural characteristics in order to further improve the membrane properties. The impact on separation performance was evaluated based on gas permeation measurements with test gases, such as He, Ar, H₂, CO₂, and CH₄, and via nitrogen adsorption to determine the membrane pore volume and internal surface area before and after steam treatment. Steam activation was shown to be an effective technique to improve membrane throughput without adversely impacting selectivity. The application of the post-treatment technique for the preparation of membranes with “reverse selectivity” appropriate for the removal of chemical warfare agents from contaminated air streams is briefly discussed as well.

1.0. INTRODUCTION

The field of nanoporous membranes for gas separations has experienced good progress during the last two decades. Currently, most of the commercial membrane-based gas separation applications use polymeric membranes. These are easily fabricated in various configurations (e.g., flat sheet, hollow fiber, etc.) and have a modest cost. On the other hand, polymeric membranes have, in general, modest separation characteristics (dictated by a permeability vs selectivity trade-off relationship¹ known as the Robeson plot) and are not, typically, intended for use under high temperatures and pressures. Carbon molecular sieve (CMS) membranes, formed by the carbonization of polymeric precursors in a controlled atmosphere (e.g., vacuum or inert gas), exhibit separation performance which often lies above the Robeson plot of competitive polymeric membranes and, in addition, show resistance to high temperatures and pressures.

During pyrolysis to prepare CMS membranes, most of the heteroatoms present in the precursor polymeric macromolecules are progressively removed, with only a cross-linked and stiff, primarily carbon skeleton structure remaining.² The pore structure of the CMS membranes is thought to be nonhomogeneous and to consist³ of both larger-pore regions, with sizes in the range of 10–20 Å (which explains the large gas permeation rates of such materials), separated by nanoporous constrictions (a few angstrom in size) that are, principally, responsible for their molecular sieving characteristics.⁴ It is such a hybrid pore structure that explains the ability of CMS membranes to perform molecular sieving type separations while

still maintaining the high-flux character of carbon materials. This group and others have produced high-quality CMS membranes in the past few years. Ismail and David⁵ reviewed some of the earlier work, and Table A in the Supporting Information section lists some of the key studies. The development of CMS membranes with the appropriate pore size characteristics has been accomplished mainly by choosing the appropriate polymeric precursor and by varying the carbonization conditions (e.g., the atmosphere, temperature and duration of pyrolysis). Often, however, the technique does not succeed⁵ to consistently provide the tight pore size control required for the separation of important gas pairs (e.g., O₂/N₂ and CO₂/CH₄), and thus, an additional post-treatment step is needed to fine-tune the pore structure of the CMS membranes. A generic “platform” post-treatment technique employed by this team is steam activation, and a systematic investigation of the approach and its application to the preparation of CMS membranes is provided here.

Though steam activation is a novel post-treatment step for membrane preparation, it is a technique used often for preparing activated carbons (AC) and other microporous materials with desired pore structures, see Table B in the

Special Issue: Baker Festschrift

Received: January 29, 2012

Revised: April 5, 2012

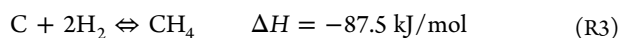
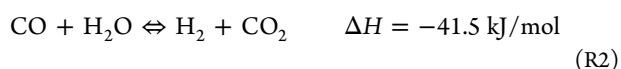
Accepted: April 5, 2012

Published: April 5, 2012

Supporting Information section for a listing of some of the key studies. During the procedure, steam reacts with carbon atoms on the internal pore surface area of the solid, and this creates additional microporosity.⁶ At some point, as the activation process continues, pore walls begin to collapse, and the number of micropores and the corresponding micropore surface area go through a maximum, and then start decreasing.⁷ At elevated temperatures, the actual process is described by the chemical reaction, R1, below:⁸



Reaction R1 has been extensively studied, not only because of its importance in the preparation of a variety of AC, but also because of its role during coal gasification. In addition to R1, other reactions that, likely, participate during the steam activation of carbons include the water–gas shift reaction R2, and the direct hydrogenation of carbon to generate methane R3.



However, it is R1 that is thought to be, primarily, responsible for the changes in the carbon pore structure during steam activation, the other reactions, likely, making minor contributions. As noted above, the phenomena taking place during steam activation are complex. The change in porosity, during the early stages of activation, is thought to result from the opening (widening) of the pore constrictions and from the development of a more interconnected pore structure. Continued reaction (“burn-off”) causes further widening of existing micropores; for CMS membranes this may originally be beneficial, as it increases the permeability, but eventually further widening of the pores, if left unchecked, will negatively impact the membrane selectivity.

The authors know of no published studies dealing exclusively with the impact of steam activation on the properties of CMS membranes; there are numerous studies, on the other hand, dealing with steam treatment as a method to prepare AC. Rodríguez-Reinoso et al.,⁹ for example, prepared AC from carbonized olive stones via steam gasification and studied the impact on porosity development of conditions like the partial steam pressure and activation temperature. They reported that activation with steam resulted in the widening of the existing micropores. Rodríguez-Reinoso et al.,⁹ reported that CO and H₂, produced via R1, act as inhibitors for R1 itself. The lower concentration of these inhibitors found in the exterior of the particles (due to diffusional limitations) favors the reaction of steam at the external particle surface. They reported that increasing the temperature from 750 to 800 °C increased the rate of R1 but also made the inhibiting effect of CO and H₂ less severe, the net result being a faster rate of porosity formation, with the maximum in porosity being displaced toward the larger burn-offs (~50%).

Molina-Sabio¹⁰ studied the steam activation of a char using immersion microcalorimetry. They reported that micropores with widths of less than 0.5 nm dominated the micropore size distribution at low burn-off levels (<10%). As the activation process proceeded, molecular sieving behavior disappeared at larger burn-off levels. In addition, only in the early stages of the activation process there was a net increase in the fraction of micropores, with micropore widening and pore “coalescence”

negatively impacting micropore volumes and surface areas at burn-off levels larger than 20% (for an activation temperature of 700 °C) and 40% (for 800 °C). Pastor-Villegas and Duran-Valle¹¹ studied the effect of activation temperature (700–950 °C) on the pore structure of steam-activated carbons from rockrose. They reported that the observed increase in the micropore volume of the carbon was mainly due to the widening of the micropores. At a 40% burn-off level, the micropore volume first increased with increasing temperature up to 850 °C (0.25 cm³/g) and, then, decreased upon further increasing to 950 °C. The maximum cumulative (mesopores plus macropores) pore volume was 0.590 cm³/g for the carbon activated at 700 °C (this volume for the starting char was 0.328 cm³/g). All the AC had a significant pore volume accessible to He (*V_p*), the maximum *V_p* = 0.957 cm³/g corresponding to the carbon activated at 700 °C at a 40% burn-off level (for the initial char *V_p* = 0.409 cm³/g).

Macia-García¹² studied the steam activation of commercial holmoak wood charcoal in a range of temperatures (800–950 °C) and burn-off levels (20–60%). The specific BET surface area (*S_{BET}*) of the resulting AC increased with increasing burn-off level, and a maximum *S_{BET}* = 987 m²/g was obtained for the sample activated at 850 °C at a 60% burn-off level (for the carbon precursor *S_{BET}* = 120 m²/g). As the burn-off level increased, so did also the micropore and mesopore volumes. For burn-off levels of 20 and 40%, the samples prepared at 850 °C had the highest micropore volume (0.241 and 0.301 cm³/g, respectively—the micropore volume of the starting precursor was 0.06 cm³/g). For the samples prepared at a 60% burn-off level, the maximum micropore volume (0.403 cm³/g) was obtained at 800 °C. Steam activation to prepare AC from walnut shells was studied by Gonzalez et al.¹³ The procedure was carried out at 700 °C for 60–120 min and at 850 and 900 °C for 30–60 min. Increasing the activation time at 850 °C from 30 to 45 min and subsequently to 60 min increased the N₂ adsorption capacity (*S_{BET}* of 699, 966, and 1361 m²/g, respectively); however, increasing the time at 700 °C had no effect on the micropore volume, and only little effect on the mesopore volume. For a time of 30 min, using different temperatures did not seem to markedly change the textural characteristics of the resulting AC. For a time of 60 min, an increase in temperature from 700 to 850 °C led to greater N₂ adsorption capacities (*S_{BET}* increased from 542 to 1361 m²/g), increased the micropore volume from 0.30 to 0.74 cm³/g, and the mesopore volume from 0.04 to 0.20 cm³/g, and also broadened the pore size distribution (PSD). A further increase in temperature to 900 °C resulted in a decrease in N₂ adsorption capacity due to micropore widening and coalescence/collapse.

Singh and Lal¹⁴ prepared AC via the carbonization of polystyrene sulfonate beads at 800 °C, followed by steam activation of the resulting chars first at 800 °C for three different times (1, 2, and 3 h) and, then, at four different temperatures (750, 800, 850, and 900 °C) for 2 h each. Increasing the time (from 1 to 3 h) resulted in an increase in *S_{BET}* (from 310 to 949 m²/g), the total pore volume (from 0.27 to 0.98 cm³/g), and in the average pore size (from 3.5 to 4.1 nm). The AC *S_{BET}* and total pore volume also increased with increasing activation temperature, with the samples exhibiting *S_{BET}* ranging from 239 to 620 m²/g and total pore volumes ranging from 0.26 to 0.62 cm³/g, when the temperature increased from 750 to 900 °C. Jaseińko-Halat and Kędzior¹⁵ studied the steam activation of bituminous coal at 750 °C for

burn-off levels of 5–25%. During the early stages of activation (burn-off levels < 10%), new micropores (~ 0.4 – 0.5 nm) were created by elimination of the constrictions present in the char, and through widening of existing micropores. These samples were reported to exhibit noticeable molecular sieving properties. At greater burn-off levels (10–25%), the formation of new micropores via the opening of constrictions came to an end, but the widening of existing micropores continued. The activation resulted in a gradual decrease (and eventually the complete disappearance) of small micropores (width < 0.41 nm), with simultaneous notable increase in the volume of larger micropores (widths 0.41 – 2.0 nm) and a slight increase in the volume of mesopores (widths 2 – 50 nm). As a result, the molecular sieving characteristics in the samples disappeared. The fraction of total micropore volume (< 2.0 nm) occupied by micropores with widths < 0.41 nm (accessible to dichloromethane and inaccessible to benzene) was 48% at a 5% burn-off level and decreased to 27% at a 25% level. The fraction of micropores with widths > 0.63 nm (accessible to tetrachloromethane) increased from 5% to 23% in the same range of burn-off levels.

In summary, the effect of steam activation on the properties of AC adsorbents has been investigated by a number of groups. The characteristics of the resulting materials have been shown to depend on the type of carbon source, the temperature and time of activation, and the burn-off level. In this paper, the focus is on the use of steam activation as a post-treatment technique in order to modify the pore size characteristics and transport and separation properties of CMS membranes. The impacts of the operating conditions, such as the temperature and period of activation, on the properties of the resulting membranes are systematically investigated.

2.0. EXPERIMENTAL PROCEDURE

The authors have been preparing CMS membranes for over ten years now^{16–20} through the controlled-atmosphere carbonization of a variety of polymeric precursors. The resulting membranes have good separation characteristics and excellent resistance to high-temperature and pressure environments.^{19,20} In fact, they are currently undergoing field-testing in coal-based power generation and in a number of other petrochemical processes. For the experimental results presented here (unless otherwise noted), polyetherimide (PEI) has been used as a polymeric precursor in the preparation of the CMS membranes; the authors have also used PEI as a model polymeric precursor in their fundamental studies of transport and separation of gas mixtures through CMS membranes.^{16–18} The PEI used in this work is Ultem1000, supplied by General Electric, and its structure is shown in Figure 1. It is a good model precursor to use as it is inexpensive, easily available, and dissolves readily in a variety of common polar solvents, a key requirement for the preparation of supported CMS membranes, which are the focus of this investigation. It prepares, in

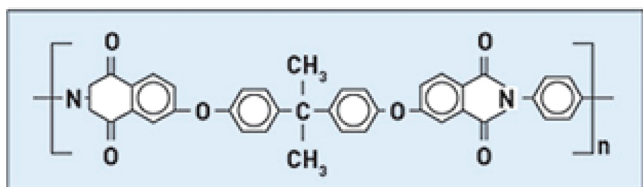


Figure 1. Ultem1000 PEI resin.

addition, CMS membranes with good permeation characteristics (high throughput and selectivity) and thermal stability, that compare favorably with membranes prepared by much more expensive and difficult to process polymeric precursors.

To prepare the supported CMS membranes in this study, ceramic tubular supports (3.5 mm ID and 6 mm OD) commercially available by Media & Process Technology, Inc. (M&P) were utilized. These are asymmetric alumina supports which are made of a relatively thick α -alumina layer on the top of which a thin layer of γ -alumina is placed via sol–gel processing. Prior to coating with the polymeric precursor (see discussion below), the ends of each substrate were glazed (using a Duncan GL Ultraclear glaze) to ensure that they are impermeable to gas transport. The quality of the resulting substrates was validated by permeation tests with He and Ar. Only substrates that exhibited good performance, with He/Ar ideal selectivities close to the Knudsen value, were selected for the preparation of CMS membranes. To prepare the coating solution, the PEI resin was dissolved in 1, 2-dichloroethane (DCE) while continuously stirring for 24 h, with a slight heating applied in the early stages of dissolution. Dip-coating solutions of different concentrations were prepared, with the more concentrated solution applied in the initial coatings, and the less concentrated solutions in the subsequent coatings (for most of the membranes in this paper use was made of two different solutions with PEI concentrations of 6 and 2 wt %, respectively).

For the substrates utilized here, the γ -alumina layer is deposited on the inside surface of the tube. To prepare CMS membranes using these substrates, their outer surface was first wrapped with Teflon tape. The substrate was then immersed in the 6 wt % PEI/DCE solution for 3 min and was subsequently withdrawn (“pulled-out”) from the solution at a constant rate of 2 cm/min, in order to coat a PEI layer with a uniform thickness on the inside (γ -alumina) surface of the tube. After coating of the PEI film, the membrane was stored in an incubator to dry for 24 h. The membrane was subsequently carbonized in a cylindrical furnace in flowing ultrahigh pure (UHP) Ar, in order to remove all the gases evolved during the pyrolysis process. The carbonization protocol involved first heating (1 °C/min) the membrane to 350 °C and holding it at that temperature for 0.5 h. The temperature was then raised (1 °C/min) to 600 °C, and the membrane was held there for an additional 4 h. Subsequently, the membrane was cooled down to 180 °C (at 2 °C/min) and further down to room temperature at a rate of 5 °C/min. The coating/carbonization procedure was then repeated a number of times (typically 3 – 4), in order to achieve the desired membrane performance (for successive coatings, as noted earlier, the 2 wt % PEI/DCE solution was utilized). The resulting CMS membranes are then ready to be subjected to additional post-treatment via steam activation.

For the steam activation step, the as prepared CMS membranes were placed in a stainless steel tubular furnace (5.1 cm in internal diameter and 60.6 cm long) and heated (1 °C/min) in the presence of UHP Ar to the preselected temperature of activation; when this temperature was reached, water was added (via an HPLC pump) to the hot flowing Ar stream to generate a (steam/Ar) mixture with a molar ratio of $2:1$. The membrane was kept in the steam/Ar flowing mixture for a predetermined period before being slowly cooled down (2 °C/min) to room temperature.

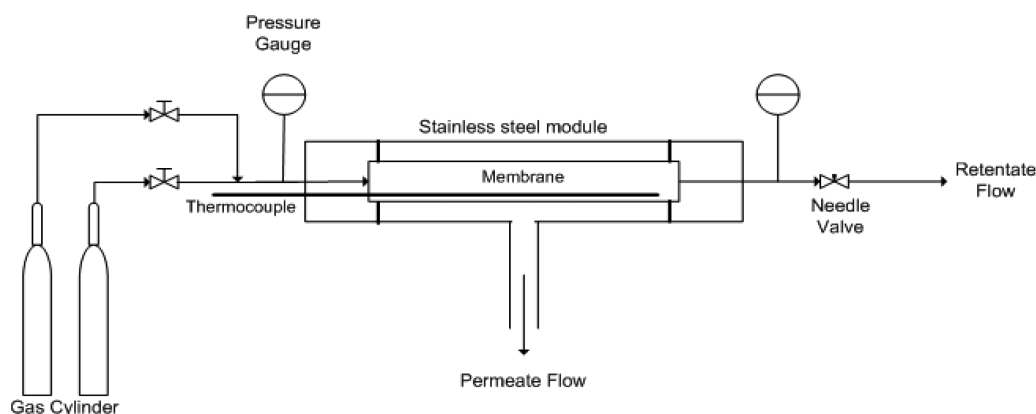


Figure 2. Schematic of the experimental apparatus.

The transport characteristics of the steam-treated membranes were determined by measuring the flux through the membrane of a number of test gases, namely He, Ar, H₂, CO₂, and CH₄. In the experiments, UHP gases were utilized, and purifier columns were used, in addition, in order to remove any water vapor or hydrocarbons, that may be present. Measurement of the permeation of He and Ar provides a good measure of the changes in the pore structure of the membranes (as it relates to their ability to separate hydrogen from its mixtures), since these two gases are noncondensable, nonadsorbing and inert, and are thus thought to interact minimally with the membrane pore surface. The other three gases (in addition to their industrial significance) provide also a measure of the changes occurring on the membrane surface in addition to information about the overall structure. During this study, only single-gas permeation tests were routinely performed. In the past, the authors have shown^{19,20} that single- and mixed-gas permeances for noncondensable gases (e.g., He, Ar, H₂, CH₄) are close to each other; and while single-gas permeation experiments are convenient to perform, as they only require the measurement of the permeate-side flow, mixed-gas permeabilities, on the other hand, they are notoriously time-consuming and difficult to measure with these high-flux nanoporous membranes and, in addition, are prone to experimental artifacts, including, but not limited to, concentration polarization effects. For the single-gas permeation experiments, the membrane was sealed inside the permeation apparatus (made of a stainless tube of the same length with appropriate end-fittings) via silicone O-rings wrapped around the glazed ends of the membrane tube. The gas was fed through the inside of the membrane tube, the pressure (~3 atm) of which was controlled by a needle valve on the tube-side outlet. The pressure on the permeate side was maintained at 1 atm. The flow rate of the outlet gas from the permeate side was measured using a soap-bubble flow meter (a schematic of the experimental apparatus and system are shown in Figure 2). On the basis of these measurements, the membrane permeances (P_j) and ideal selectivities (S_{ij}) were calculated by the following equations:

$$P_j = \frac{VT_o P_m}{T_m P_o \Delta P 2\pi RL} \quad (1)$$

$$S_{ij} = \frac{P_i}{P_j} \quad (2)$$

where V is the volumetric flow rate (m³/h) of the gas across the membrane, P_m is the pressure (bar) at which the volumetric

flow of permeate side was measured, T_m is the temperature (K) where the measurements were taken, L is the membrane length (m), R is the membrane inner radius (m), P_o and T_o are the pressure (bar) and temperature (K) at standard conditions, and ΔP (bar) is the pressure difference across the tube.

3.0. RESULTS AND DISCUSSION

3.1. Permeation Studies. In this study steam activation is utilized as a post-treatment step in order to adjust the pore structure characteristics to produce CMS membranes with the desirable selectivity and permeation properties. A key advantage of steam activation is that it is a relatively "gentle" technique (when compared to alternate post-treatments to modify the pore structure such as air oxidation or direct hydrogenation), that provides an effective control of the pore size and structure (see results to follow) via the reaction of steam with the carbon surface but has a minimal impact on the membrane surface and mechanical properties. In this section, the experimental findings of the effect of steam activation on the properties of the treated CMS membranes are discussed.

Figure 3 illustrates the effect of the temperature and the period of steam activation on the membrane permeation characteristics. Two different CMS membranes were utilized in these experiments, prepared by the preparation protocol described previously. Their permeation characteristics (He and Ar permeances at 120 °C) were measured prior to steam activation and were shown to be similar. Note, that as the He and Ar permeances in Figure 3 indicate, these two particular membranes (though microporous based on their sorption characteristics, see discussion to follow) are not permselective, potentially due to the presence of a few pinholes and "cracks"—for CMS nanoporous membranes even a small number of such "imperfections" severely degrade the selectivity. Both these membranes were subsequently subjected to steam activation for 1 h, the first membrane at 600 °C, and the other at 700 °C. After the steam treatment, the membranes were slowly cooled down to room temperature, and their He and Ar permeances were measured at 120 °C. After the first set of permeation measurements, the membranes were again placed in the steam-treatment furnace and were further activated for one additional hour, then cooled down to room temperature, and their He and Ar permeances measured once more at 120 °C. This (activation/permeation measurement) protocol was repeated several times, and the resulting experimental data are shown in Figure 3. The temperature of activation and the duration of the treatment are the two most important

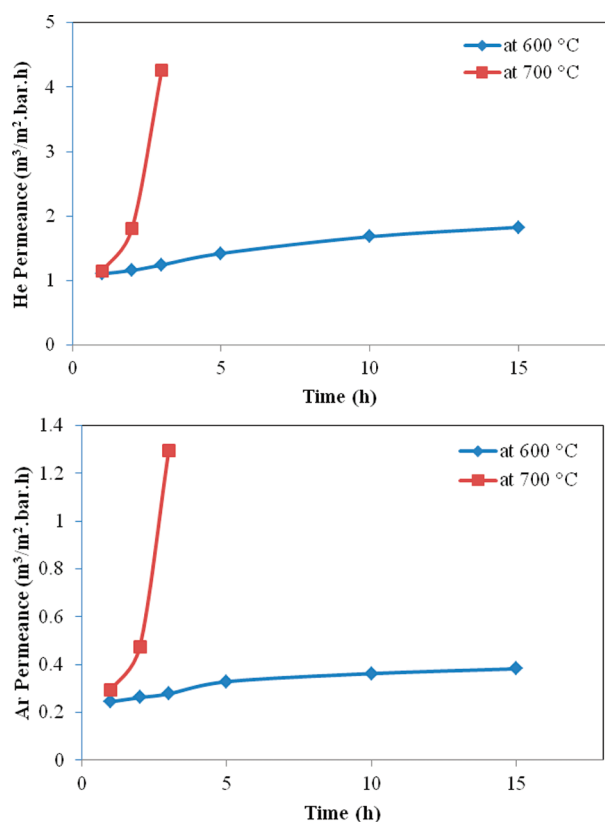


Figure 3. Permeance of membranes as a function of temperature and time of steam activation: (top) He permeance, (bottom) Ar permeance.

parameters at one's disposal for adjusting the pore size characteristics of CMS membranes via steam activation. As expected, higher temperatures of activation result in accelerated increases in the membrane permeance; and though this may be beneficial from a processing standpoint (a decrease in the post-treatment time needed), it also presents unique challenges in terms of properly controlling the final pore structure characteristics.

The results in Figure 3 are of value as they show the impact of steam activation on Ar permeance, and the effect of the process conditions (e.g., time of treatment and temperature of activation). The presence of pinholes in the two membranes in Figure 3 tends, unfortunately, to mask the impact of steam activation on membrane selectivity. Figure 4 depicts the impact of steam activation on the permeation characteristics of a selective CMS membrane, also prepared via the pyrolysis of the same PEI precursor but by following a slightly modified pyrolysis protocol. Specifically, the membrane was heated-up to 450 °C (with a heating rate of 1 °C/min) and held there for 4 h. Its temperature was then raised to 700 °C (0.5 °C/min), held there for 8 h, and subsequently, the membrane was cooled down to 25 °C (1 °C/min). This membrane was again subjected to steam activation following the same (activation/permeation measurement) protocol as the membranes in Figure 3, first at 600 °C for a number of hours, and subsequently at 700 °C for an additional period. As with the membranes in Figure 3, temperature and duration of the activation treatment are shown once more to be key operating parameters. Note also, that steam activation provides for a delicate control of the pore structure and permeation properties of the treated membranes. For the (He/Ar) gas pair, steam

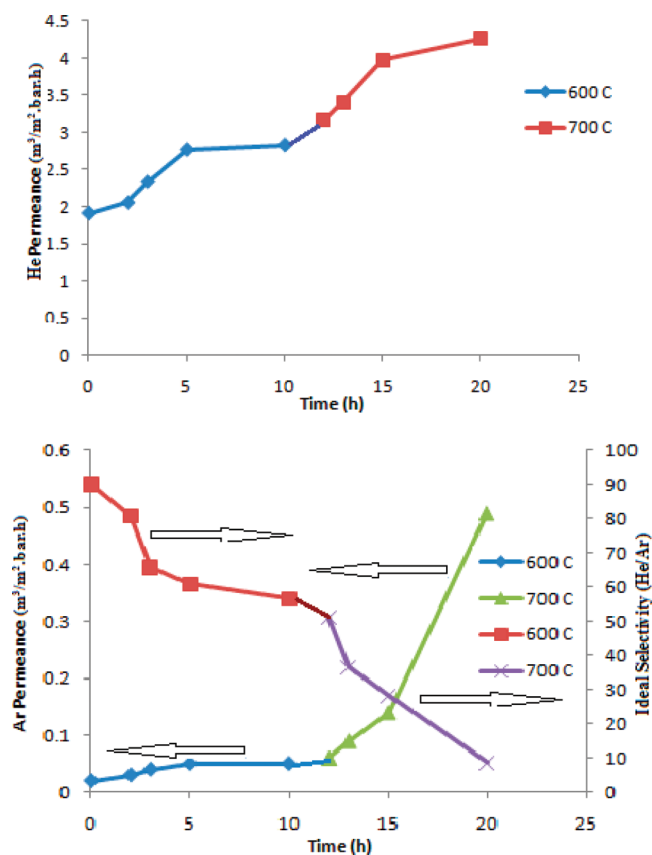


Figure 4. Permeance of membranes as a function of temperature and time of steam activation: (top) He permeance; (bottom) Ar permeance and ideal selectivity.

treatment results in a monotonic decrease in the ideal selectivity. This is not always the case, however, with other gas pairs, which show different behavior (see further discussion to follow); this is a manifestation of the complex phenomena that govern membrane transport through such nanoporous membranes.

As noted above, the impact of steam activation on the permeation properties of a given membrane is a sensitive function of the membrane's starting pore structure, but also of the gas-pair with which one chooses to probe the impact of steam post-treatment. To study these issues, four CMS membranes were prepared via the controlled-temperature pyrolysis of three PEI top layers deposited on the top of M&P alumina supports, following the preparation protocol described previously. Prior to the initiation of the steam activation, the single-gas permeation properties of this group of membranes were measured at 120 °C using three different test gases, specifically H₂, CO₂, and CH₄. Table 1 shows the experimental data. Despite the fact that all membranes were prepared using the same preparation protocol, there is still some variability (i.e., range of values) in the measured transport properties (11% in the hydrogen permeance, 24.5% in the CO₂ permeance, and 18% in the methane permeance). This variability in properties (albeit, from what we know, in line with what is "feasible" in the area of CMS and inorganic supported membranes) is attributed to the variability in the properties of the initial substrates (for example, the thickness and quality of the top γ -alumina layer) that determine to a great extent the fraction of pinholes and "cracks" in the final membrane sample. The four CMS membranes were sub-

Table 1. H₂, CO₂, and CH₄ Permeances (m³/m²·bar·h) and Ideal Selectivities of Four Three-Layer CMS Membranes Prior to Steam Treatment

	membrane 1	membrane 2	membrane 3	membrane 4
P_{H_2}	0.514	0.457	0.492	0.479
P_{CO_2}	0.138	0.183	0.163	0.158
P_{CH_4}	0.023	0.028	0.024	0.027
$S(H_2/CO_2)$	3.7	2.5	3.0	3.0
$S(H_2/CH_4)$	22.7	16.3	20.5	17.7

sequently subjected to 6 h of steam treatment at 600 °C, after which their permeation properties were measured. The membranes were subsequently subjected to three additional cycles of steam treatment (6 h each), followed by single-gas permeation tests at 120 °C. Figure 5 shows the permeances of

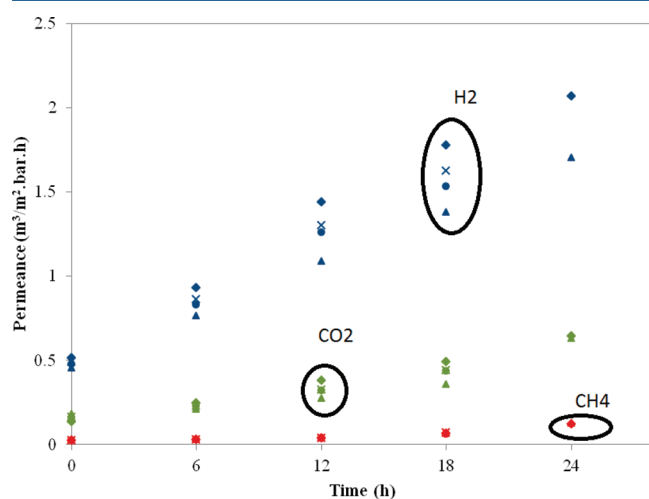


Figure 5. H₂, CO₂, and CH₄ permeances of four different membranes as a function of the duration of steam treatment: H₂ blue ♦ (M₁), ▲ (M₂), × (M₃), ● (M₄); CO₂ green ♦ (M₁), ▲ (M₂), × (M₃), ● (M₄); CH₄ red ♦ (M₁), ▲ (M₂), × (M₃), ● (M₄), where M_n indicates membrane number *n*.

H₂, CO₂, and CH₄, while Figure 6 shows the corresponding ideal H₂/CO₂ (Figure 6 top) and H₂/CH₄ (Figure 6 bottom) selectivities. In agreement with the experimental findings utilizing the He/Ar gas pair (see Figures 3 and 4), the permeances of all gases increase with the post-treatment time

The behavior shown in Figure 5 is qualitatively consistent with what is known from the literature on activated carbons, (see prior discussion) about the mechanism of steam activation, which is thought to remove carbon atoms from the interior membrane surface (via R1), resulting thus in the enlargement of the micropores and the opening to gas transport of previously closed (inaccessible) pore regions. However, the impact of steam activation on the membrane separation characteristics (in terms of the ideal selectivities of select gas pairs, shown in Figure 6) is substantially more complex. For the H₂/CO₂ pair, for example, for some of the membranes it remains fairly unaffected by steam treatment, while for others a maximum in the separation selectivity is clearly observed. This interesting nonmonotonic (with respect to the time of activation) behavior of the ideal selectivity is present in all four membranes for the H₂/CH₄ gas pair. For all these membranes, the ideal H₂/CH₄ selectivity initially increased

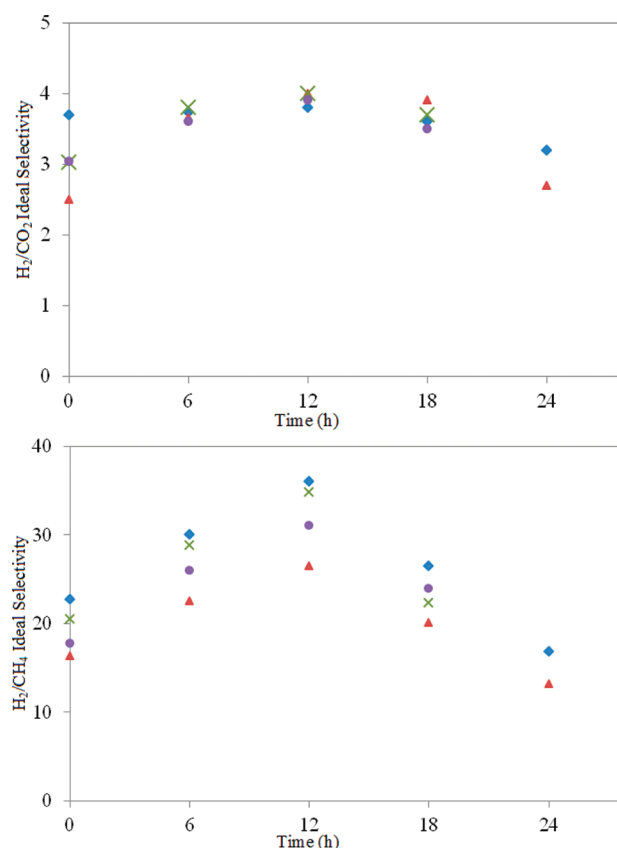


Figure 6. Ideal H₂/CO₂ (top) and H₂/CH₄ (bottom) membrane selectivities as a function of the period of steam activation. The symbols correspond to various membranes as follows: ♦ (M₁), ▲ (M₂), × (M₃), ● (M₄).

after the treatment. This is probably due to initial growth of the microporosity of the pore network, which impacts more significantly the H₂ rather than the CH₄ flux through the membrane, consistent with the idea that the latter gas has more limited access to (and mobility inside) that region of the pore space. As the activation time further increases, the ideal H₂/CH₄ selectivity goes through a maximum and eventually begins to decline. This behavior is consistent with the idea that in the early stages of the steam activation process, there is a net creation of microporosity resulting in the modified membranes exhibiting higher gas permeances without loss in selectivity; further steam processing, however, causes a widening of the narrow micropores (potentially converting some of them into mesopores), and resulting thus in a loss in selectivity, and in the diminishing of the molecular sieving characteristics of the treated membranes. However, as already noted, the selectivity behavior for the H₂/CH₄ gas pair is different from that of the He/Ar pair shown in Figure 4. That the (He/Ar) ideal selectivity does not follow similar behavior is interesting but not totally unexpected behavior, however, as He and Ar have access to different parts of the pore-space than H₂ and CH₄. Nevertheless, the mechanism that explains the membrane selectivity behavior in Figure 6 notwithstanding, a key observation here is that steam activation provides potentially an effective route to simultaneously improve the molecular sieving characteristics as well as the throughput (permeance) of these membranes.

3.2. Adsorption Studies. Studying the transport characteristics of the CMS membranes prior to, as well as following the

steam activation step provides valuable information regarding the separation mechanisms of these systems and the various phenomena that occur during the steam post-treatment procedure. In the present study, the transport investigations have been complimented with parallel ones of the sorption characteristics of the same materials. Adsorption/desorption measurements using probe gases (in this study N_2 at its liquid temperature) provide good insight into the pore structure characteristics, including the membrane internal surface area and the pore volume accessible to the probe gas. Combined with an appropriate geometric (or molecular) model of the membrane's pore structure (e.g., a 3-D network created by a Voronoi tessellation^{21,22}), they can also provide valuable insight into the geometry and topology of the pore structure itself. It should be noted here, that though transport and sorption measurements provide complementary information about the membrane pore space, they each provide information about unique aspects of the pore space as well. For example, sorption experiments are thought to access the "totality" of the pore-space; transport measurements, on the other hand, "sample" only the flow-through porosity.

The nitrogen sorption experiments were carried out at 77 K (the liquid temperature of nitrogen) in a static mode using a commercial system (ASAP 2010 Micropore Analyzer from Micromeritics, Inc.). This system is equipped with a UHV pump that was used to degas the membrane sample (and the overall sorption system) down to 10^{-5} Torr (the degassing step, carried out at 250 °C, lasted typically about 24 h). As noted above, though measuring the amount of nitrogen that adsorbs (and desorbs) from the membrane sample and calculating the total surface area and total pore volume are rather straightforward tasks, extracting additional structural information (e.g., average pore size and PSD) is much dependent upon selecting the appropriate geometric (or molecular) model of the pore space. The latter step is rather complicated and involves elaborate simulations that go beyond the scope of the present investigation. Here instead, commonly employed techniques (the so-called BJH method for the mesoporous region, and the Horvath–Kawazoe (HK) method for the microporous region) were utilized to extract additional structural information from the nitrogen adsorption data. Since these methods make use of substantial simplifying assumptions (e.g., the HK method assumes the material's pore structure to consist of slit-like pores), it is the qualitative trends in the various structural parameters (e.g., average pore diameters) that are more important rather than their exact values.

A good "base-line" measurement, when working with supported CMS membranes, is that of the starting support material itself on which the permselective membrane layers are deposited. Figure 7 presents the PSD data of one of the substrates, based on experimental sorption data and calculated using the BJH method. For these ceramic substrates, with an asymmetric pore structure, gas adsorption mainly takes place in the γ -alumina top layer, whose weight is only a small fraction of the total weight of the support substrate;¹⁷ as a result, the values reported for the cumulative and differential pore volumes are low, due to the fact that the total weight of the support tube is used in the calculation. The PSD analysis indicates an average pore diameter for the mesoporous layer between 4 and 5 nm, which is consistent with what the literature typically reports for sol–gel γ -alumina layers, and also the average pore diameter this group measures from transport data with the same support tubes.

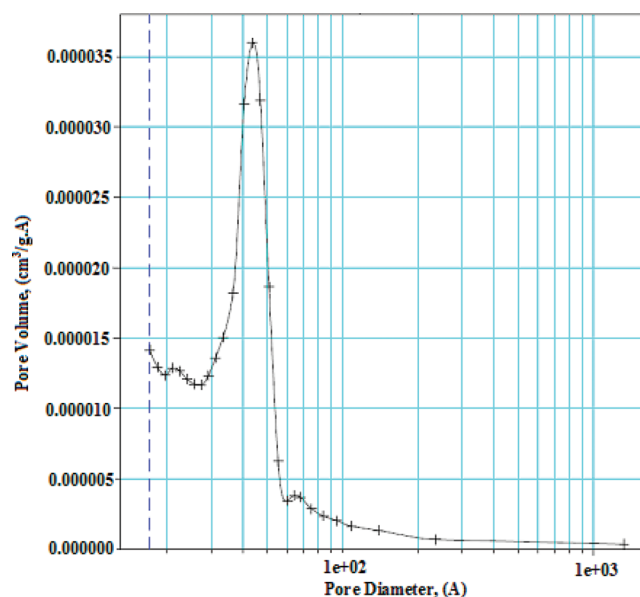


Figure 7. Pore size distribution of the support substrate.

A CMS membrane was prepared by depositing on this substrate three carbon layers following the preparation protocol previously described. The single-gas permeances for H_2 , CO_2 , and CH_4 of the supported CMS membrane were measured prior to steam activation, and are shown in Table 2. In Figure 8

Table 2. H_2 , CO_2 , and CH_4 Permeances and Ideal Selectivity of a Three-Layer CMS Membrane before Steam Activation

permeance ($m^3/m^2 \cdot bar \cdot h$)				selectivity
H_2	CO_2	CH_4	H_2/CO_2	H_2/CH_4
3.138	0.763	0.108	4.1	29.0

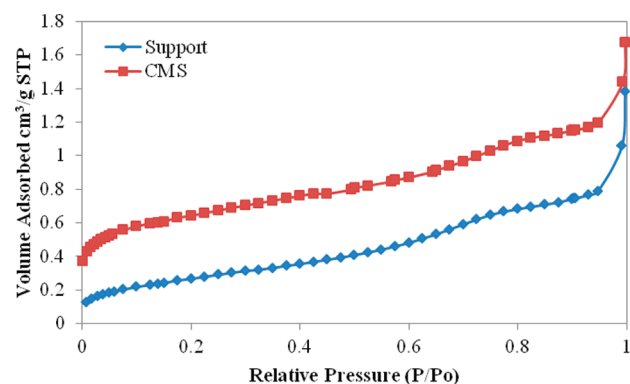


Figure 8. Nitrogen adsorption isotherm of the support substrate and the CMS membrane.

the adsorption isotherm (volume of gas adsorbed per g of sample as a function of relative pressure) for this CMS membrane is compared with that of the original support substrate. Clearly, the addition of the carbon layers has led to a greater N_2 adsorption capacity and, most importantly, has endowed the supported membrane with molecular sieving behavior, as shown in Table 2.

This CMS membrane was subsequently exposed to steam activation at 600 °C for 6 h and, then, cooled down to room temperature inside the furnace. The membrane was then inserted into the sample module of the sorption apparatus, and

its nitrogen adsorption isotherm was measured following the steam treatment. The same procedure of steam activation for 6 h, then followed by measurement of the adsorption isotherm repeated three additional times, for a total period of steam activation of 24 h. The top figure in Figure 9 depicts the N_2

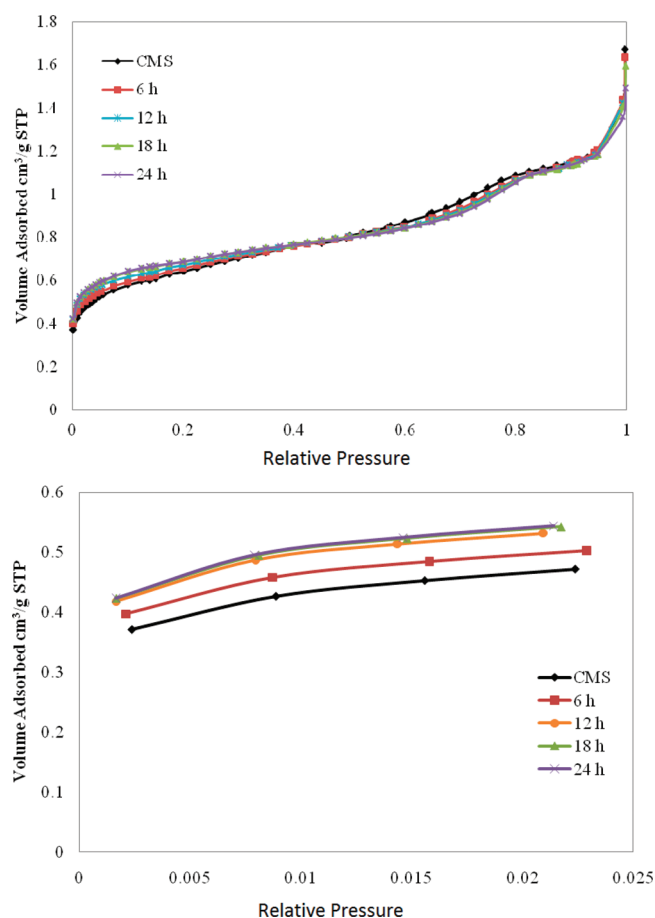


Figure 9. Nitrogen adsorption isotherms of the CMS membrane steam activated for various periods: (top) the whole relative pressures region; (bottom) the low relative pressure region.

adsorption isotherms of the original CMS membrane together with the isotherms of the membrane after it had been subjected to several cycles of steam activation (6, 12, 18, and 24 h). All the isotherms, shown in that figure, are a combination of types I and II, according to the IUPAC classification of physisorption isotherms, with the type I isotherm reflecting the presence of the microporous carbon layers, and the type II isotherm mostly reflecting the mesoporous γ -alumina top layer of the ceramic membrane support, but also some of the mesoporosity of the carbon layers.

As the results in the top of Figure 9 indicate, the isotherm shapes do not change significantly even after 24 h of activation at 600 °C, signaling the continued presence of a substantially microporous carbon layer. As the bottom of Figure 9, which shows the expanded portion of the isotherm in the low relative P/P_0 range (up to 0.03), indicates during the initial stage of the activation (from 0 to 12 h) the adsorption of nitrogen increases significantly. Conventionally, nitrogen adsorption in this low relative pressure region is thought to reflect the influence of the micropores,⁶ and an increase in nitrogen adsorption, therefore, signals the creation of additional microporosity. Further steam

activation (from 12 to 24 h) results in a substantially smaller increase in the adsorption capacity (bottom in Figure 9), signaling no significant further increase in the number of micropores formed.

The adsorption data in the microporous region were further analyzed by the HK method, and Figure 10 shows the effect of

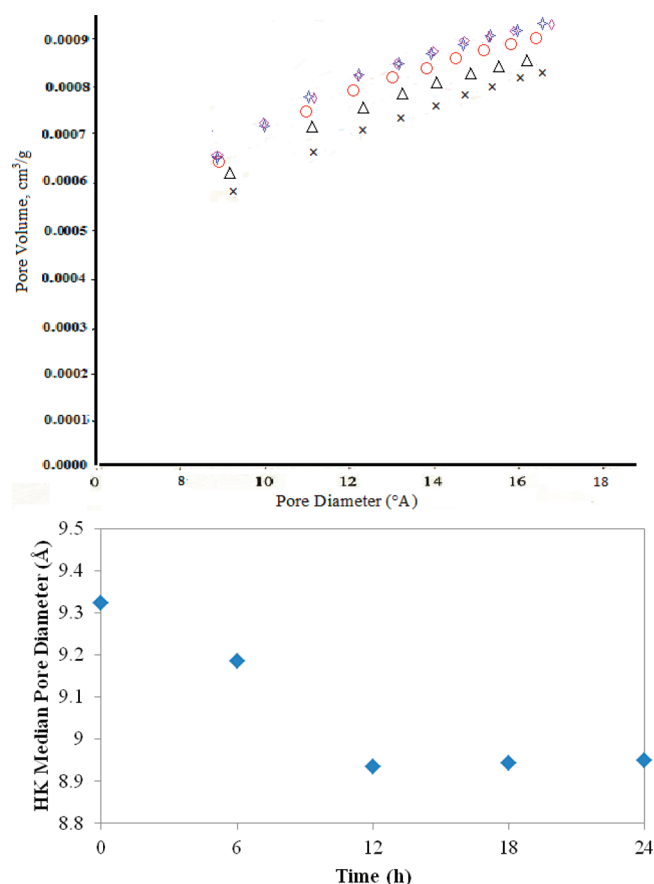


Figure 10. (top) HK cumulative pore volume plots of steam-activated CMS membrane for various activation times where \times (CMS), Δ (6 h), \circ (12 h), \diamond (18 h), \star (24 h). (bottom) Corresponding HK median pore diameters.

steam activation on PSD and the average pore diameter as a function of the time of steam treatment. The results in the top of Figure 10 show that the micropore volume increases with increasing time of activation, the most significant increase occurring in the first 12 h of the activation. The reason for the increase in the micropore volume is likely due to the widening of existing narrow micropores, but also due to the development of new micropores; the latter phenomenon is manifested in the bottom of Figure 10, where one observes a decrease in the median pore diameter in the microporous region. However, the increase in the micropore volume (and the decrease in the median pore diameter) slows down in the latter stages of activation, from 12 to 24 h. Interestingly enough, during the same period of steam activation (0–24 h), BJH analysis of the adsorption data indicates a decrease of the mesopore volume and an increase in the average pore diameter (see Figure 11). The data in Figure 10 are consistent with the data in Figures 4–6 that indicate an increase in the permeance of hydrogen (and He) without loss in the separation performance for short to medium times of steam activation. Reaction with steam over

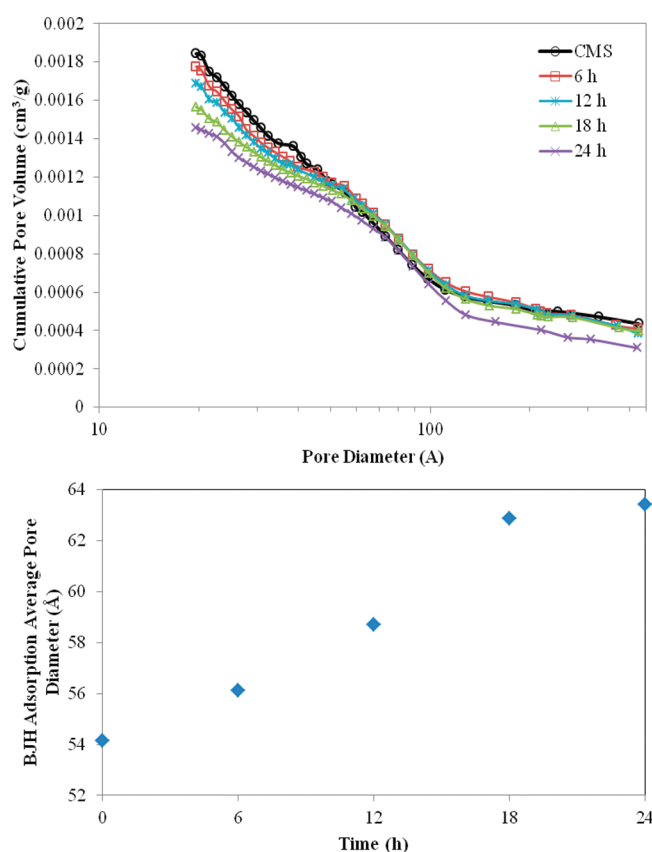


Figure 11. (top) BJH cumulative pore volume plots of steam-activated CMS membrane for various activation times. (bottom) Corresponding BJH average pore diameters.

a longer period of time leads to the formation of “cracks” and pinholes that cause a loss in the molecular sieving character of CMS.

3.3. Surface-Flow Membranes. One important application of the technique of steam activation is the preparation of CMS membranes appropriate for use in a surface-flow based membrane separator (SFMS). This concept, which was originally proposed for the separation of condensable vapors from refinery streams,²³ is currently being tested by the authors for the removal of chemical warfare agents (CWA) from contaminated air streams. In the collective protection (CP) device, this team is investigating, the SFMS precedes a Knudsen-flow membrane reactor (KFMR) which catalytically oxidizes the CWA,²⁴ with the SFMS serving the role to reduce the toxin load on the KFMR, particularly during peak-level periods. The authors are also investigating the use of such SFMS with toxic industrial chemicals (TIC), and, if needed, for incorporating additional separation functionality into the CP device for the removal of potentially harmful by-product (e.g., NH₃, HCl, etc.) from the KFMR stage.

During surface-flow membrane separation, the CWA condenses within the membrane structure to make it impermeable to air flow, transports through the membrane via liquid flow and re-evaporates on the permeate side (such behavior is also known as “reverse selectivity”²³). Initial efforts, so far, with the removal of dimethyl methylphosphonate (DMMP), which is known as a chemical precursor (and used to simulate its characteristics) for Sarin (GB), a toxic CWA, point out the critical importance of optimizing the membrane’s structural characteristics. For example, CMS membranes with

small average pore size showed inferior performance, as DMMP plugged completely their pore structure and, at least under the conditions the authors investigated, the sweep air flow was not able to efficiently remove the CWA from the membrane structure. Large-pore membranes, on the other hand, resulted in large air-loss, which is an undesirable outcome. As a result, steam activation has provided a very effective means for optimizing membrane performance for the proposed application. The technique can be used to tailor the pore size of the CMS membrane to an appropriate value required for achieving desired adsorption/pore condensation characteristics for a given target compound. An additional key advantage of the proposed post-treatment approach, as it relates to the eventual large-scale production of the proposed CP device, is that it can be executed on a module basis, while simultaneously maintaining precise control of the degree of pore structure tuning by online monitoring.

Figure 12 depicts the He and N₂ permeances of one the CMS membranes utilized in the SFMS studies (this membrane

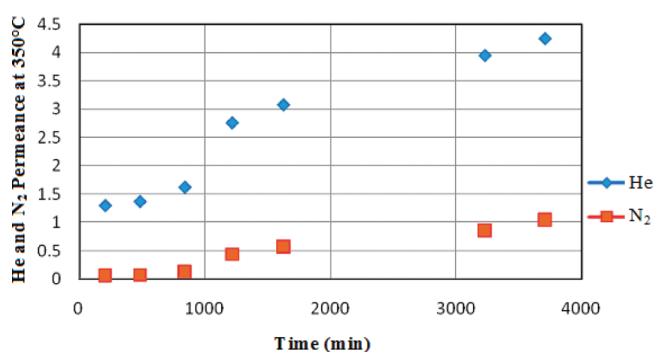


Figure 12. He and N₂ permeance of the membrane as a function of the time of steam activation.

is prepared by M&P on the aforementioned tubular ceramic substrate using a proprietary blend of phenol formaldehyde novolac resin-based polymer precursors and carbonized under similar conditions as the membranes described above) as it is being subjected to steam activation. Both the He and N₂ permeances increase with activation, similar to the behavior shown in Figures 3 and 4 for He and Ar. As Figure 12 indicates, upon completion of the steam treatment, the membrane is no longer permselective. However, it is still fairly microporous as indicated by the activated transport of He at the higher temperatures (see Table 3). When tested with pure CO₂

Table 3. He and N₂ Permeances of a Steam-Treated CMS Membrane

temperature [°C]	N ₂ permeance [m³/m²·bar·h]	He permeance [m³/m²·bar·h]
350	1.04	4.25
250	1.16	4.07
150	1.37	4.00
80	1.45	3.89

(which is used as a convenient to use model gas to test the membrane’s ability to function as a SFM for CWA removal), the gas completely condenses and fills the membrane structure (as manifested by the leveling-off of its flux) at a fairly low pressure P_e ($P_e/P_{\text{sat}} = 0.07$). Unfortunately, the pore size of the resulting membrane is too small for the membrane to function

as an effective SFMS for DMMP removal. Upon exposure to DMMP, the pore structure completely plugged, and the sweep air flow was not able to efficiently remove the CWA from the membrane structure. Membranes prepared using the same precursor following similar carbonization methods, but subjected to more “aggressive” steam post-treatment (higher temperature), have been shown effective in SFMS for the removal of DMMP, as Figure 13 indicates which depicts the

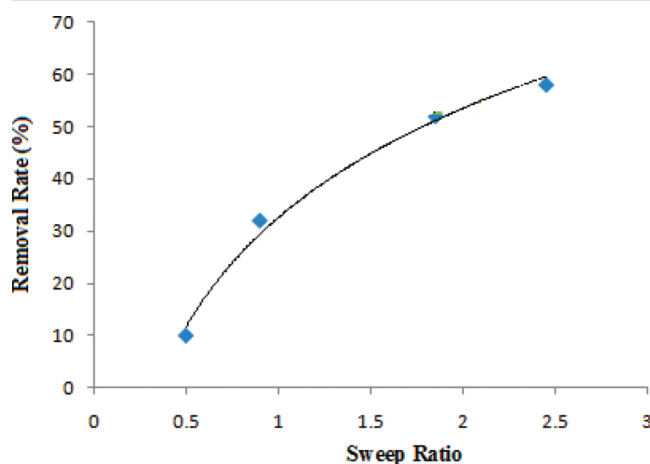


Figure 13. DMMP removal rate via a surface-flow membrane; $T = 50^\circ\text{C}$, $\Delta P = 0.71\text{--}0.74$ bar, DMMP concentration = 303–311 ppm.

DMMP removal rate from contaminated streams using one such membrane (different from the one in Figure 12).

4.0. CONCLUDING REMARKS

A systematic investigation was performed aiming to assess the effectiveness of steam activation as a post-treatment technique for fine-tuning the pore size characteristics and separation properties of CMS membranes. The steam activation procedure was shown to be effective in modifying the membrane internal pore structure, as evidenced by changes in the measured permeances and ideal selectivities of the membranes treated. The temperature of activation and the duration of the treatment were determined to be two important parameters one could adjust in order to attain desirable pore size characteristics and better membrane performance. It was also shown that by choosing the right temperature of activation, and by appropriately manipulating the duration of treatment, one can sensitively adjust the average pore size of the CMS membranes without diminishing their separation performance. Key advantages of steam activation are its ease of application, and the fact that it is a relatively gentle technique that allows one to simultaneously increase a membrane's throughput and selectivity without negatively impacting its mechanical properties. The technique has also proven very effective in the preparation of membranes for SFMS applications for the removal of CWA and TIC from contaminated air streams. One key advantage of the steam activation approach for the latter application (but also for the more conventional gas-phase applications) is that it can be executed on a modular basis, while simultaneously maintaining precise control of the degree of pore structure tuning by online monitoring.

■ ASSOCIATED CONTENT

⑤ Supporting Information

Table A lists some of the key prior studies on the preparation of CMS membranes, and Table B describes a few of the most notable investigations on the use of steam activation for the preparation of activated carbons. This material is available free of charge via the Internet at <http://pubs.acs.org/>.

■ AUTHOR INFORMATION

Corresponding Author

*Tel.: 213 740 2069. Fax: 213 740 8053. E-mail address: tsotsis@usc.edu.

Notes

The authors declare no competing financial interest.

■ ACKNOWLEDGMENTS

This research was made possible by financial support from the Defense Threat Reduction Agency (DTRA) under Project Number: BB10PHM201. Useful discussions with Dr. Charles Bass, Mr. William Buechter, and Ms. Tracee Harris of DTRA and Dr. Richard Ciora of Media and Process Technology, Inc., are gratefully acknowledged. Some of the early aspects of this work were also supported by the California Energy Commission.

■ REFERENCES

- (1) Singh, A.; Koros, W. J. Significance of entropic selectivity for advanced gas separation membranes. *Ind. Eng. Chem. Res.* **1996**, *35*, 1231–1234.
- (2) Lagorsse, S.; Magalhaes, F. D.; Mendes, A. Carbon molecular sieve membranes sorption, kinetic and structural characterization. *J. Membr. Sci.* **2004**, *241*, 275–287.
- (3) Koresh, J.; Abrahams, S. Study of molecular sieve carbons. Part 1: Pore structure gradual pore opening and mechanism of molecular sieving. *J. Chem. Soc., Faraday Trans I* **1980**, *76*, 2457–2471.
- (4) Centeno, T. T.; Fuertes, A. B. Supported carbon molecular sieve membranes based on phenolic resin. *J. Membr. Sci.* **1999**, *160*, 201–2011.
- (5) Ismail, A. F.; David, L. I. B. A review on the latest development of carbon membranes for gas separation. *J. Membr. Sci.* **2001**, *193*, 1–18.
- (6) Bansal, R. C.; Donnet, J. B.; Stoeckli, H. F. *Active carbon*; Marcel Dekker: New York, 1988.
- (7) Walker, P. L., Jr. Production of activated carbons: Use of CO_2 versus H_2O as activating agent. *Carbon* **1996**, *34*, 1297–1299.
- (8) Menéndez-Díaz, J. A.; Martín-Gullón, I. Types of carbon adsorbents and their production. *Act. Carb. Surf. Envir. Remed.* **2006**, *7*, 1–47.
- (9) Rodríguez-Reinoso, F.; Molina-Sabio, M.; González, M. T. The use of steam and CO_2 as activating agents in the preparation of activated carbon. *Carbon* **1995**, *33*, 15–23.
- (10) Molina-Sabio, M. Effect of steam and carbon dioxide activation in the micropore size distribution of activated carbon. *Carbon* **1996**, *34*, 505–509.
- (11) Pastor-Villegas, J.; Duran-Valle, C. J. Pore structure of activated carbons prepared by carbon dioxide and steam activation at different temperatures from extracted rockrose. *Carbon* **2002**, *40*, 397–402.
- (12) Macias-Garcia, A. Preparation of active carbons from a commercial holm-oak charcoal: Study of micro- and meso-porosity. *Wood. Sci. Technol.* **2004**, *37*, 385–394.
- (13) Gonzalez, J. F.; Román, S.; González-García, C. M.; Valente Nabais, J. M.; Luis, O. A. Porosity development in activated carbons prepared from walnut shells by carbon dioxide or steam activation. *Ind. Eng. Chem. Res.* **2009**, *48*, 7474–7481.
- (14) Singh, A.; Lal, D. Preparation and characterization of activated carbon spheres from polystyrene sulphonate beads by steam and carbon dioxide activation. *J. App. Poly. Sci.* **2010**, *115*, 2409–2415.

- (15) Jaseińko-Halat, M.; Kędzior, K. Comparison of molecular sieve properties in microporous chars from low-rank bituminous coal activated by steam and carbon dioxide. *Carbon* **2005**, *43* (5), 944–953.
- (16) Sedigh, M. G.; Onstot, W. J.; Xu, L.; Peng, W. L.; Tsotsis, T. T.; Sahimi, M. Experiments and simulation of transport and separation of gas mixtures in carbon molecular sieve membranes. *J. Phys. Chem. A* **1998**, *102*, 8580–8589.
- (17) Sedigh, M. G.; Xu, L.; Tsotsis, T. T.; Sahimi, M. Transport and morphological characteristics of polyetherimide-based carbon molecular sieve membranes. *Ind. Eng. Chem. Res.* **1999**, *38*, 3367–3380.
- (18) Sedigh, M. G.; Jahangiri, M.; Liu, P. K. T.; Sahimi, M.; Tsotsis, T. T. Structural characterization of polyetherimide-based carbon molecular sieve membranes. *AIChE J.* **2000**, *46*, 2245–2255.
- (19) Abdollahi, M.; Yu, J.; Liu, P. K. T.; Ciora, R.; Sahimi, M.; Tsotsis, T. T. Hydrogen production from coal-derived syngas using a catalytic membrane reactor based process. *J. Membr. Sci.* **2010**, *363*, 160–169.
- (20) Abdollahi, M.; Yu, J.; Liu, P. K. T.; Ciora, R.; Sahimi, M.; Tsotsis, T. T. Process intensification in hydrogen production from syngas. *Ind. Eng. Chem. Res.* **2010**, *49*, 10986–10993.
- (21) Rajabbeigi, N.; Elyassi, B.; Tsotsis, T. T.; Sahimi, M. Molecular pore-network model for nanoporous materials. I: Application to adsorption in silicon carbide membranes. *J. Membr. Sci.* **2009**, *335*, 5–12.
- (22) Rajabbeigi, N.; Elyassi, B.; Tsotsis, T. T.; Sahimi, M. Molecular pore-network model for nanoporous materials. II: Application to transport and separation of gaseous mixtures in silicon carbide membranes. *J. Membr. Sci.* **2009**, *345*, 323–330.
- (23) Rao, M. B.; Sircar, S. Nanoporous carbon for separation of gas mixtures by surface flow. *J. Membr. Sci.* **1993**, *85*, 253–264.
- (24) Motamedhashemi, M. Y.; Egolfopoulos, F.; Tsotsis, T. T. Application of a flow-through catalytic membrane reactor (FTCMR) for the destruction of a chemical warfare simulant. *J. Membr. Sci.* **2011**, *376*, 119–131.